International Journal of Automotive Technology, Vol. 11, No. 3, pp. 331–337 (2010)
DOI 10.1007/s12239–010–0041–1

1229–9138/2010/052–05

EFFECT OF VEHICLE MODEL ON THE ESTIMATION OF LATERAL VEHICLE DYNAMICS

J. KIM*

Department of Vehicle Dynamics Research Team, Hankook Tire Co., LTD., R&D Center, 23-1 Jang-dong, Yuseong-gu, Daejeon 305-725, Korea

(Received 14 August 2008; Revised 26 October 2009)

ABSTRACT–A methodology is presented for estimating vehicle handling dynamics, which are important to control system design and safety measures. The methodology, which is based on an extended Kalman filter (EKF), makes it possible to estimate lateral vehicle states and tire forces on the basis of the results obtained from sinusoidal steering stroke tests that are widely used in the evaluation of vehicle and tire handling performances. This paper investigates the effect of vehicle-road system models on the estimation of lateral vehicle dynamics in the EKF. Various vehicle-road system models are considered in this study: vehicle models (2-DOF, 3-DOF, 4-DOF), tire models (linear, non-linear) and relaxation lengths. Handling tests are performed with a vehicle equipped with sensors that are widely used by vehicle and tire manufacturers for handling maneuvers. The test data are then used in the estimation of the EKF and identification of lateral tire model coefficients. The accuracy of the identified values is validated by comparing the RMS error between experimentally measured states and regenerated states simulated using the identified coefficients. The results show that the relaxation length of the tire model has a notable impact on the estimation of lateral vehicle dynamics.

KEY WORDS : Extended kalman filter, Tire lateral force, Magic formula, Vehicle model

1. INTRODUCTION

Mathematical models describing the lateral dynamics of road vehicles are being extensively used in the simulation and design of modern vehicles in order to improve their handling performance. The main source of uncertainty in these models is due to the interaction between the tires and the road surface because of the non-linear dependence of the lateral forces on several variables such as longitudinal slip, sideslip angle, normal load, camber angle, tire pressure, temperature, wear and road surface characteristics.

Notable attempts have been made to work out both analytical tire force models based on physical principles as well as empirical models such as Pacejka's Magic Formulas (Bakker and Pacejka, 1989). Analytical models are usually difficult to handle and require an accurate knowledge of tire component parameters, which are hardly measurable or identifiable in practice. Conversely, in the empirical models suggested by Pacejka, tire forces are described by a family of curves whose coefficients are identified from experimental laboratory tests (Bakker and Pacejka, 1989). However, these methods have limitations in representing real tire force characteristics due to conditions that are different from road tests. Therefore, the need for correction arises, which can be made only through tests performed in real conditions, i.e., on the road. In addition, a suitable elaboration of the measurements is required.

Some identification and observation methodologies have been suggested to solve this problem. For example, Kiencke and Daiβ (1997) and Stephant *et al.* (2007) present linear and non-linear observation using a bicycle model. Mancosu and Speziari (1999) and Bolzern *et al.* (1999) suggest the use of the EKF method to determine the tire lateral force on the basis of a pre-established theoretical model and the results of experimental tests performed on a corresponding real model. It is therefore necessary to define a mathematical model and have access to the real system and its experimental results. The estimations can be made using an identification technique after reproducing the results of the real system using the theoretical model. Therefore, the more complete the mathematical model is, the closer the obtained values will be to the real ones. Although this will require a great deal of computational load, it will produce a model that will be able to use the identified results to make a comprehensive analysis of the vehicle's dynamics. On the other hand, if the model is simplified, the identified results will be less close to the real values. This will entail a lighter computational work load, but the model will only enable analysis of a limited field of the vehicle's operating conditions, namely those used for its identification. It is therefore necessary to first define the objective in order to choose the most fitting model and consequently, the identification technique.

The goal of this manuscript is to offer a simple and

**Corresponding author.* e-mail: jskim89@kaist.ac.kr

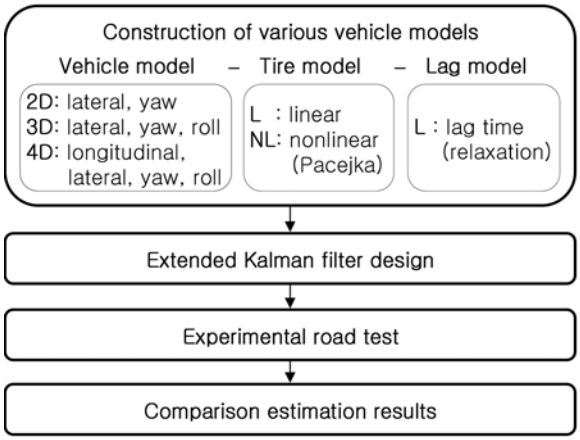

Figure 1. Overall work flow to analyze the effect of the vehicle model on lateral tire force estimation.

reliable vehicle model for the identification of lateral vehicle dynamics and tire forces. The overall working procedure of this paper is shown in Figure 1. First, three different kinds of vehicle-road system models are constructed: vehicle model, tire model and lag model. In the vehicle model, various degrees of freedom of the model are considered, for example 2D (lateral, yaw), 3D (lateral, yaw, roll) and 4D (longitudinal, lateral, yaw, roll). In the tire model, L (linear) and NL (non-linear Pacejka) models are considered. In the lag model, time delay of tire lateral force with relaxation lengths is considered. As a result, various kinds of vehicle-road system models can be constructed by the combination of vehicle-tire-lag model. Then, the EKF is designed for the various vehicle models. The techniques are based on the continuous EKF and make it possible to set up the lateral tire forces so that they reproduce the vehicle's behavior not only in the maneuvers used for identification but also for any other maneuver. Experimental road tests for handling maneuvers are performed to obtain the measurement data from a real vehicle. These data are used in the off-line estimation of the EKF. Finally, the comparison of EKF estimation with respect to the various vehicle-road system models is performed. The accuracy of the estimation is validated by comparing the RMS value of error between experimentally measured states and regenerated states simulated using the identified coefficients.

2. CONSTRUCTION OF VEHICLE MODELS

The mathematical vehicle-road system model used for the identification procedure can have a maximum of four degrees of freedom accounting for longitudinal displacements, lateral displacements, yaw and roll rotations as shown in Figure 2. Assuming a moving reference system attached to the vehicle and considering the longitudinal velocity v_x, lateral velocity v_y, yaw rate r, roll angle ϕ and roll rate p as state variables, the equation of motion becomes:

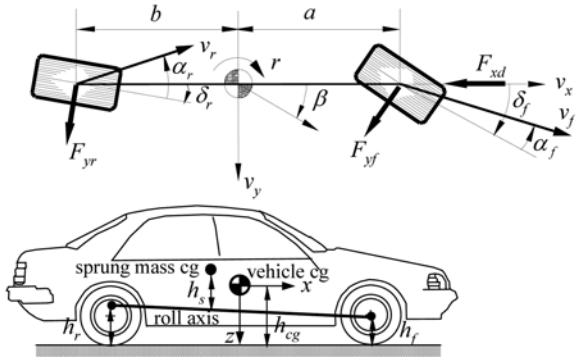

Figure 2. Mathematical vehicle-road system model.

$$
\begin{aligned}
&m\dot{v}_x = mv_y r - F_{yf}\sin\delta_f - F_{yr}\sin\delta_f - F_{xd}\\
&m\dot{v}_y + m_s h_s \dot{p} = -mv_x r + F_{yf}\cos\delta_f + F_{yr}\cos\delta_r\\
&I_{zz}\dot{r} - I_{xzs}\dot{p} = aF_{yf}\cos\delta_f - bF_{yr}\cos\delta_r\\
&\dot{\phi} = p\\
&I_{xxs}\dot{p} + m_s h_s \dot{v}_y - I_{xzs}\dot{r} = -m_s h_s v_x r\\
&\qquad + m_s g h_s \sin(\phi) - L_\phi \phi - L_p p
\end{aligned} \tag{1}
$$

$$\dot{F}_{yf} = \frac{v_x}{\sigma_f}(-F_{yf} + \bar{F}_{yf})$$

$$\dot{F}_{yr} = \frac{v_x}{\sigma_r}(-F_{yr} + \bar{F}_{yr})$$

where m is the total vehicle mass, m_s is the sprung mass i.e., the mass supported by the suspension and I_{zz} is the moment of inertia of the entire vehicle around the vertical axis, I_{xxs} is the moment of inertia of the sprung mass around the longitudinal axis, I_{xzs} is the inertia product of the sprung mass and L_ϕ and L_p are total roll stiffness and damping, respectively. Moreover, a and b are the distances from centre of gravity of the vehicle to the front and rear axles and h_s is the distance from the roll axis to the centre of gravity of the sprung mass. F_{xd} is the equivalent longitudinal drag force due to aerodynamics, rolling resistance and so forth. Also, F_{yf} and F_{yr} are the transient lateral tire force on the front and rear wheels, respectively. In general, these forces are primarily functions of the related slip angle α_i, dynamic normal loads Z_i, camber angles γ_i and longitudinal slip s_i ($i=f, r$). The lateral tire force values F_{yi} can be evaluated from the steady-state lateral tire force $\bar{F}_{yi}$ introducing the relaxation lengths σ_i. The load transfer, which is responsible for fluctuations of the normal loads, can be approximated by a static function of the lateral forces themselves (Bolzern *et al*., 1999). With these hypotheses, it is possible to view the lateral tire forces only as a function of the slip angle, as follows:

$$\bar{F}_{yi} = \bar{F}_{yi}(\alpha_i, Z_i(\bar{F}_{yi}))\,. \tag{2}$$

Equation (1) only includes steering input and ignores the effect of other inputs such as the road-bank angle. Therefore, the estimation will be obtained by observing the vari-

ation in the state output due to steering input perturbations only. When a road-bank angle exists, it is necessary to include an accurate road-bank estimation algorithm in the model in order to estimate lateral forces accurately as suggested by Tseng (2001). In this study, the road-bank angle is assumed to be zero.

In the model shown in Figure 2, it is easy to recognize that the front and rear slip angles α_f and α_r are obtained as a function of the independent variables as follows:

$$\alpha_f = -(\delta_f + \varepsilon_f \phi) + \tan^{-1}\left(\frac{v_y + ar}{v_x}\right)$$

$$\alpha_r = -\varepsilon_r \phi + \tan^{-1}\left(\frac{v_y - br}{v_x}\right) \quad (3)$$

where δ_f is the steer angle, which can be obtained by dividing the steering wheel angle δ_h by an overall steering gear ratio of the steering gear box. Also, ε_f and ε_r are front and rear roll steer coefficients, which include roll steer effects in the vehicle model. The model shown in Equation (1) is convenient for the theoretical analysis of vehicle dynamics as explained by Wong (2001). By this advantage, automobile engineers can easily understand the handling characteristics of vehicle.

There exist two distinct kinds of tire models. The first, the linear model, can be adopted when driving well within the limit of adhesion. From the linear model, the lateral tire forces can be expressed as the following:

$$\bar{F}_{yi}(\alpha_i) = K_i \alpha_i, \; i = f, r \quad (4)$$

where K_i is the cornering stiffness of the tire. The second, non-linear model can be applied when the vehicle approaches the physical limit of adhesion. In order to reproduce the non-linear relationship between slip angles and steady-state tire lateral forces, the following so-called Magic formulas are adopted (Bakker and Pacejka, 1989):

$$\bar{F}_{yi}(\alpha_i) = D_i \sin\left[C_i \tan^{-1}\{B_i\alpha_i - E_i(B_i\alpha_i - \tan^{-1}(B_i\alpha_i))\}\right], \; i = f, r \; . \quad (5)$$

As is well known, the parameters in Equation (5) have a direct interpretation as follows. Specifically, C is a shape factor that is usually fixed to 1.3, D indicates the peak value of the force and E determines the curvature at the peak value. Note that the product BCD represents the initial slope and corresponds to the linearized cornering stiffness. Equations (1), (3), (4) and (5) are the vehicle-road system models used in the estimation of vehicle handling dynamics.

3. EKF DESIGN

As the road test gives the time history of only a few system states, it is necessary to deduce all other states in order to identify the vehicle parameters. Therefore, a technique based on the Kalman filter has been adopted due to its high reliability as a state and parameter observer simultaneously.

The identification technique adopted here, namely the continuous extended non-linear Kalman filter, calls for the model and the measurements to be available in the form of continuous functions of time. It is thus necessary to have measurements sampled at a sufficiently high frequency so that the measurements can be made continuous during algorithm execution through linear interpolation.

Letting $x(t)$ be the state vector, such that

$$\mathbf{x}(t) = [v_x(t)\; v_y(t)\; r(t)\; \phi(t)\; p(t)\; F_{yf}(t)\; F_{yr}(t)]^T \quad (6)$$

and $u(t) = \delta_f(t)$ be the measured input variable, the model of the vehicle can be described by Equation (1) and the kinematics relations of Equation (3) and the expression of the equivalent suspension-tire axle lateral forces of Equations (4)~(5). The vehicle model can then be written in a compact form as:

$$\dot{\mathbf{x}}(t) = \mathbf{f}(\mathbf{x}(t),\, u(t),\, t) \; . \quad (7)$$

Assuming that the geometric and inertial parameters are known, the uncertainties are restricted to the parameters appearing in the tire model of Equations (4)~(5) and to the relaxation lengths. Longitudinal drag force, F_{xd} can be determined using a set of sensors that does not require direct measurement. A second-order random walk model is appended in order to model the longitudinal drag force to be determined:

$$\begin{bmatrix} \dot{y}_0 \\ \dot{y}_1 \end{bmatrix} = \begin{bmatrix} 0 & 1 \\ 0 & 0 \end{bmatrix} \begin{bmatrix} y_0 \\ y_1 \end{bmatrix} + \mathbf{w}_y \quad (8)$$

where y_0 represents the force to be determined, y_1 is its first time derivative and $\mathbf{w}_y$ is random white noise. Thus, in the problem of estimating the lateral tire force F_{yi} of Equation (1), it is necessary to identify the steady-state lateral tire force F_{yi} of Equation (2) and the relaxation length σ_i of Equation (1). Therefore, if the non-linear tire model of Equation (5) is used, the vector of parameters $\mathbf{p}$ to be identified is given by:

$$\mathbf{p} = [B_f\; D_f\; E_f\; B_r\; D_r\; E_r\; \sigma_f\; \sigma_r\; F_{xd}\; \dot{F}_{xd}]^T \; . \quad (9)$$

In order to use an EKF for the identification of the unknown parameters, the augmented state vector is defined as:

$$\underline{\mathbf{x}}(t) = \begin{Bmatrix} \mathbf{x}(t) \\ \mathbf{p}(t) \end{Bmatrix} . \quad (10)$$

If the parameters appearing in Equation (5) and the relaxation lengths are constant with time, then Equation (7) can be written as:

$$\begin{aligned} \dot{\underline{\mathbf{x}}}(t) &= \underline{\mathbf{f}}(\underline{\mathbf{x}}(t), t) + \mathbf{w}(t) \\ \underline{\mathbf{z}}(t) &= \underline{\mathbf{h}}(\underline{\mathbf{x}}(t), t) + \mathbf{v}(t) \end{aligned} \quad (11)$$

where $\mathbf{w}(t)$ is a random zero-mean process as in Gelb (1974). The process-noise matrix describing the random process $\mathbf{w}(t)$ for is given by $\mathbf{Q}(t) = \mathrm{E}[\mathbf{w}(t)\mathbf{w}(t)^{\mathrm{T}}]$. Also, $\mathbf{v}(t)$ is a zero-mean random process described by the measurement noise matrix $\mathbf{R}(t)$, which is defined as $\mathbf{R}(t) = \mathrm{E}[\mathbf{v}(t)\mathbf{v}(t)^{\mathrm{T}}]$.

The vectors $\underline{\mathbf{x}}$ and $\underline{\mathbf{f}}$ have the following structure:

$$\underline{\mathbf{x}}(t)=\begin{bmatrix} x_1(t) \\ x_2(t) \\ \cdots \\ x_7(t) \\ \hline p_1 \\ p_2 \\ \cdots \\ p_8 \\ \hline p_9(t) \\ p_{10}(t) \end{bmatrix}, \quad \underline{\mathbf{f}}(t)=\begin{bmatrix} f_1(\underline{\mathbf{x}}(t),t) \\ f_2(\underline{\mathbf{x}}(t),t) \\ \cdots \\ f_7(\underline{\mathbf{x}}(t),t) \\ \hline 0 \\ 0 \\ \cdots \\ 0 \\ \hline \underline{x}_{17}(t) \\ 0 \end{bmatrix} \tag{12}$$

in which $x_i(t)$ indicates the seven states in Equation (6) and p_i indicates the parameters that have to be identified. Consequently, the first seven terms in the vector $\underline{\mathbf{f}}(t)$ are deduced from Equation (7), whereas the middle part of the vector contains some zeroes to impose the fact that the parameters do not vary over time. The third part is constructed from the random walk model of Equation (8). The overall size n of the two vectors is given by the sum of the seven system states and the ten parameters to be identified.

The vector $\mathbf{z}(t)$ of the measurements has a size m equal to the number of quantities recorded during a test. In the most general case, the vector is dependent on the system state through the non-linear relation $\mathbf{h}(\mathbf{x}(t), t)$. Having posed the problem in the form described above, the value of the ten parameters p_i together with the estimate of the seven states x_i is provided by the steady state solution of the following system of first order differential equations:

$$\begin{aligned} \dot{\hat{\underline{\mathbf{x}}}}(t) &= \underline{\mathbf{f}}(\hat{\underline{\mathbf{x}}}(t),t)+\mathbf{K}(t)\left[\underline{\mathbf{z}}(t)-\underline{\mathbf{h}}(\hat{\underline{\mathbf{x}}}(t),t)\right] \\ \dot{\mathbf{P}}(t) &= \mathbf{F}(\hat{\underline{\mathbf{x}}}(t),t)\mathbf{P}(t)+\mathbf{P}(t)\mathbf{F}^T(\hat{\underline{\mathbf{x}}}(t),t) \\ &\quad +\mathbf{Q}(t)-\mathbf{P}(t)\mathbf{H}^T(\hat{\underline{\mathbf{x}}}(t),t)\mathbf{R}^{-1}(t)\mathbf{H}(\hat{\underline{\mathbf{x}}}(t),t)\mathbf{P}(t) \\ \mathbf{K}(t) &= \mathbf{P}(t)\mathbf{H}^T(\hat{\underline{\mathbf{x}}}(t),t)\mathbf{R}^{-1}(t) \end{aligned} \tag{13}$$

where the matrices $\mathbf{F}$ and $\mathbf{H}$ are given by:

$$\begin{aligned} \mathbf{F}(\hat{\underline{\mathbf{x}}}(t),t) &= \left[\frac{\partial \underline{\mathbf{f}}(\underline{\mathbf{x}}(t),t)}{\partial \underline{\mathbf{x}}(t)}\right]_{\underline{\mathbf{x}}(t)=\hat{\underline{\mathbf{x}}}(t)} \\ \mathbf{H}(\hat{\underline{\mathbf{x}}}(t),t) &= \left[\frac{\partial \underline{\mathbf{h}}(\underline{\mathbf{x}}(t),t)}{\partial \underline{\mathbf{x}}(t)}\right]_{\underline{\mathbf{x}}(t)=\hat{\underline{\mathbf{x}}}(t)}. \end{aligned} \tag{14}$$

Considering that the estimate error covariance matrix $\mathbf{P}$ is symmetrical and only the terms of the main diagonal and one of the two triangles need to be calculated, the number of differential equations in the system (13) is given by: $N=n+(n\cdot n-n)/2+n=(n^2+3n)/2$. In the present study, the solution of the system of N differential equations (13) was obtained by adopting the Runge-Kutta method, starting with known initial conditions for the state and approximated conditions for the parameters and terms of the matrix $\mathbf{P}$. At each step of the integration, the terms of the $\mathbf{F}$ and $\mathbf{H}$ matrices need to be updated by numerically executing the derivatives in Equation (14).

For each road test performed, a file of data is generated containing the time history of the steering wheel input δ_h and measurement outputs of longitudinal speed, lateral acceleration and yaw rate, $\mathbf{z}(t)=[v_x \ a_y \ r]$. These data facilitate the beginning of an integration cycle for the system from Equation (13), starting from initial time t=0. The integration proceeds by interpolating the data up to the final time corresponding to the end of the maneuver. During integration, the values assumed by the unknown parameters are stored and are averaged at the end. The averaged values thus obtained are used as input values for a further integration cycle and the described procedure is reiterated until the estimated parameter values have stabilized. For the estimation problem of the 4D-NL-L model of Figure 1, there are seven states and three measurements and ten parameters have to be identified. Therefore, the number N of simultaneous differential equations required by the system from Equation (13) is equal to 170. The size of the $\mathbf{F}$ matrix is 17×17 and that of the $\mathbf{H}$ matrix is 3×17. Therefore, at each step of the identification process 17×17 +3×17=340 numerical derivatives of Equation (14) must be computed. Nevertheless, considerations of the structure of the model equations make it possible to greatly reduce the number of numerical derivatives that must be computed actually, as most of the terms in the $\mathbf{F}$ and $\mathbf{H}$ matrices can be calculated analytically.

4. COMPARISON ESTIMATION RESULTS

The first step of the proposed methodology is to acquire measurements during road tests with a vehicle. Sinusoidal steering stroke with a magnitude of 90 degrees is implemented for this purpose. Three quarters of sinusoidal steering with a magnitude of 90 degrees are applied at first. The steering wheel is then held in a constant position for 0.5 seconds and finally made to undergo the last quarter of the sinusoidal steering. This test is chosen because it is severe enough to cover a non-linear range of sideslip angles and rapid enough to represent transient behavior of vehicle-road system.

The vehicle is set-up with a steering robot to enable application of the commanded steering angle during the test and measure the steering wheel torque and angle. Vehicle motions are recorded with a combined IMU (Inertial measurement unit)/GPS (Global position system) that enable the motion of the vehicle to be recorded and presented with regards to various reference frames, including the vehicle body frame of reference and a global set of axes as shown in Figure 3. During the sinusoidal steering stroke test (with the procedure described above), several vehicle state signals are recorded, including lateral acceleration a_y, yaw r and roll rate p, vehicle speed v_x and lateral velocity v_y. The results are shown in Figure 4.

Filter tuning requires selection of an appropriate disturbance spectral density that is associated with noise $\mathbf{w}(t)$. Although the exact amount of process noise to be used is often determined experimentally, a good starting point is

Figure 3. Installation of combined IMU/GPS system in vehicle.

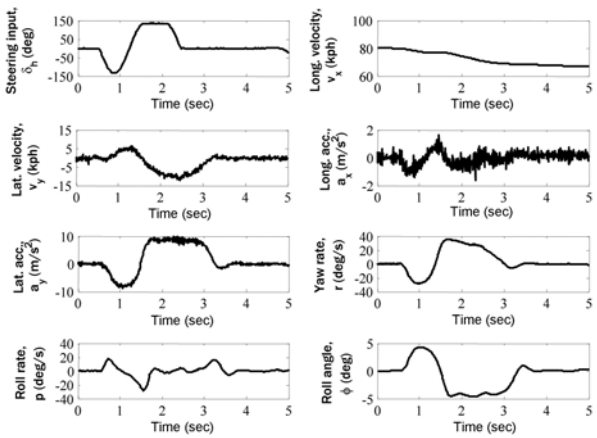

Figure 4. Measurement data used during the estimation phase: sinusoidal steering stroke maneuver (135 degree).

one where the amount of process noise reflects the designer's estimate of the lack of knowledge of the real world. Therefore, in order to determine the process noise of unknown parameters, the uncertainty in the expected initial error in the estimate is squared and divided by the amount of filtering time. The expected initial error is set as 5% of the initial value. In the process noise of $F_{xd}(t)$ and its derivative, large values are required for acceptable force transient response. This term is chosen as 250,000 for each

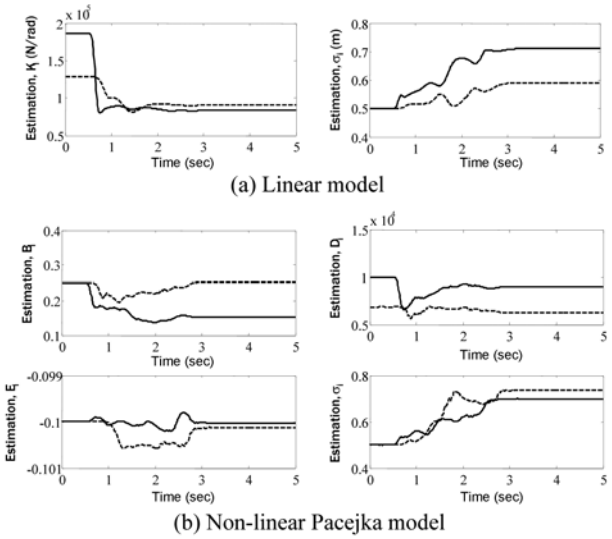

Figure 5. Identified values of tire model parameters and relaxation lengths: front (solid) and rear (dashed).

value. Independent white noise sources are added to the measurement data with RMS (root mean square) values of 0.27 m/s, 1.0 m/s^2 and 0.03 rad/s on the v_x, a_y and r, respectively. For consistency, these magnitudes are similar to those experienced within the car test experiment and are similar to the noise levels applied in the noise covariance matrix design process.

4.1. Parameter Estimation

The time histories of the parameters of tire models that are estimated off-line in the EKF are shown in Figure 5. The parameters appearing in Equations (4)~(5) and relaxation

Table 1. Parameter values of tire lateral force characteristics in the linear model.

Axle	Relaxation length (m)	Cornering stiffness (N/rad)
	σ	K
Front (i=f)	0.72 (±0.0062)	83522.29 (±303.32)
Rear (i=r)	0.59 (±0.0083)	90974.52 (±378.55)

Table 2. Parameter values of tire lateral force characteristics in the non-linear Pacejka model.

	Magic formula parameters $\overline{F}_{yi}(\alpha_i)=D_i\sin[C_i\tan^{-1}\{B_i\alpha_i-E_i(B_i\alpha_i-\tan^{-1}(B_i\alpha_i))\}]$				Relaxation length (m)	Cornering stiffness (N/rad)
Axle	**B**	**C**	**D**	**E**	σ	**K**
Front (i=f)	0.153 (±0.0027)	1.3 –	9029 (±91.9)	−0.100 (±6.18E-5)	0.700 (±0.0076)	102761 (±938.6)
Rear (i=r)	0.252 (±0.0017)	1.3 –	6268 (±34.32)	−0.100 (±5.49E-5)	0.736 (±0.0076)	117838 (±349)

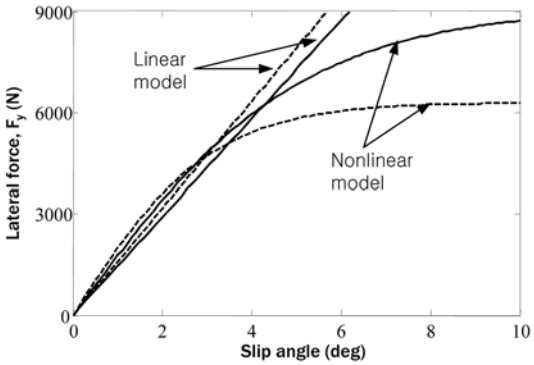

Figure 6. Lateral tire forces generated with the identified parameters-front (solid) and rear (dashed).

lengths reach steady-state values an approximately four seconds. The parameter values are determined by averaging the estimates obtained during the steady-state. The results are shown in Tables 1~2 (averaged over 50 simulation runs). The present vehicle shows understeer tendency, which is evident from the cornering stiffness, which shows an understeer gradient of approximately 0.034 deg/g.

The lateral tire forces related to the front and rear axles have been generated by applying the identified parameters to Equations (4)~(5). The results are shown in Figure 6. It can be seen that there are large differences between linear and non-linear tire model characteristics.

4.2. EKF Evaluations

After plugging the estimated parameters into the vehicle model of Equation (1), vehicle states can be reconstructed. The identified parameter values have been validated by comparing the regenerated states with the corresponding measured values. Figure 7 shows the comparisons of v_y, r and a_y states according to the change of vehicle model used in the EKF. The regenerated states are found to be fairly close to the measured data. By comparing the RMS error between regenerated states and measurements, we find that the errors can be reduced by changing the vehicle model from 2D-NL-L to 3D-NL-L. In contrast, it can be seen that the RMS errors are similar between 3D-NL-L and 4D-NL-L and appear to be independent of the longitudinal motion in the EKF.

Figure 8 shows the state comparisons according to the change of tire model used in the EKF. It shows that all filters estimate yaw rate extremely well. Analytically, this phenomenon is reasonable because the non-linearity of the

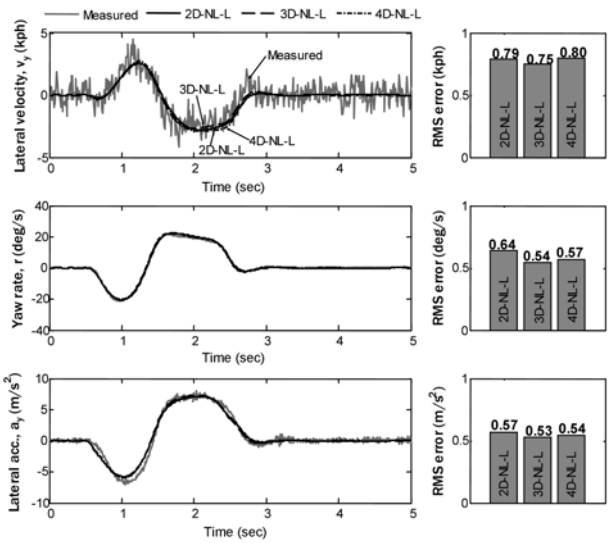

Figure 7. Comparison between experimental measurement and simulation data for different vehicle models.

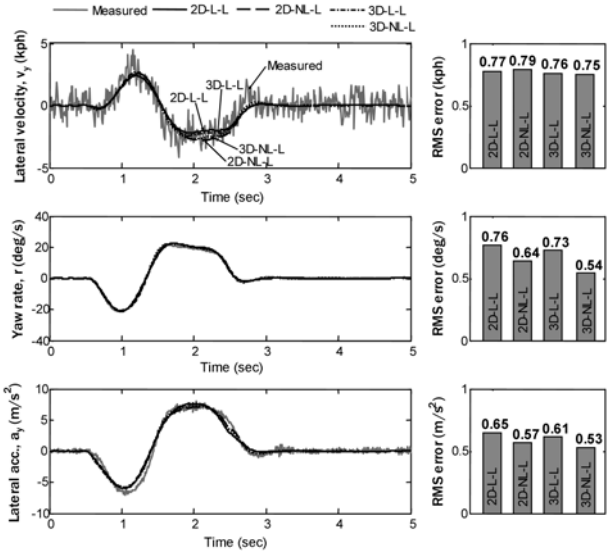

Figure 8. Comparison between experimental measurement and simulation data for different tire models.

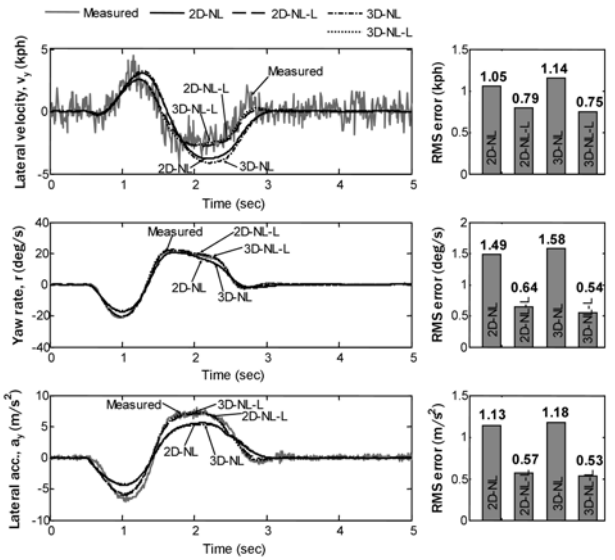

Figure 9. Comparison between experimental measurement and simulation data for relaxation length.

vehicle model in the r state is relatively insensitive to the tire non-linearity, which, in the vehicle model, has the highest non-linearity effect. From Equation (1), it can be shown that yaw dynamics are strongly affected by lateral tire forces. However, as the overall yaw moment is the difference between the lateral tire force moments at the front and rear wheels, the overall non-linearity affected by lateral tire force is reduced. The highest non-linearity effect occurs in sideslip velocity dynamics. Equation (1) shows that sideslip velocity is actually caused by the addition of four lateral tire forces. As a result, it is strongly influenced by tire non-linearity. As can be seen in Figure 8 of the v_y state, all filters show adequate estimations in mild maneuver regions where lateral acceleration is low. The estimation in severe maneuver regions, where lateral acceleration is high, are classified into two groups by the tire model used: (2D-L-L, 3D-L-L) and (2D-NL-L, 3D-NL-L). Also, the RMS errors of the non-linear tire model (2D-NL-L, 3D-NL-L) are smaller than those of the linear model (2D-L-L, 3D-L-L), especially in the r and a_y states. This result shows that the estimation accuracy of the EKF is improved due to the use of the non-linear tire model.

Figure 9 shows the effect of lateral tire force lag on the estimation accuracy of the EKF. The effects are not subtle. The regenerated state responses of v_y, r and a_y cannot be adequately characterized without considering the relaxation lengths in the vehicle-road system model. This result also shows the importance of lateral tire force lag in the EKF estimation to capture all features of the vehicle dynamics. In general, these effects are most pronounced at lower speeds and higher frequencies of steer input. The fast response shown in Figure 9 illustrates this very well; if the relaxation length is neglected (2D-NL, 3D-NL), there is a big difference between the regenerated state response and the measurement in v_y, r and a_y.

5. CONCLUSION

This manuscript proposes a procedure to identify the lateral tire forces imparted to the axles based on a simple vehicle model and experimental road data. Three kinds of vehicle-road systems for the EKF are considered: vehicle models (2D, 3D, 4D), tire models (linear, non-linear) and lag models (relaxation length). The 3D-NL-L and 4D-NL-L models are able to represent the measured states v_y, r and a_y for a sinusoidal steering stroke with a magnitude of 90 degree driving, compared to the 2D-NL-L model. However, there is no significant improvement in EKF parameter estimation by including longitudinal motion. The 3D-NL-L and 2D-NL-L non-linear tire models in the EKF are capable of representing the measured states v_y, r and a_y in a wide range of lateral acceleration variation, particularly in severe situations. The linear models (2D-L-L, 3D-L-L) are not satisfactory when lateral acceleration is significant. At high acceleration levels, the linear assumption has limitations and is unable to take non-linear tire behavior into account. In particular, it shows that relaxation length has a notable impact on the estimation accuracy of the EKF. Therefore, it is recommended that relaxation length, which is a transient characteristic of the tire, should be considered in the estimation of lateral vehicle dynamics.

The results of this study may be useful in providing road-adaptability to vehicle stability control systems such as ESP (Electronic Stability Program) and VDC (Vehicle Dynamic Control). In addition, the suggested method can be applied to the analysis of vehicle handling performance. Therefore, it is possible to provide engineers with an exact instructions for the improvement of vehicle and tire handling performance with respect to vehicle dynamics (Kim, 2008). Future studies will evaluate and improve vehicle-road system models in order to widen validity domains for various vehicle maneuvers.

ACKNOWLEDGEMENT–This research is supported by the R&D centre of HANKOOK Tire Co., Ltd., under the Kontrol technology program. The author also thanks the Vehicle Dynamics Research Team for providing field test data and valuable suggestions.

REFERENCES

Bakker, E. and Pacejka, H. B. (1989). A new tire model with an application in vehicle dynamics studies. *SAE Paper No*. 890087.

Bolzern, P., Cheli, F., Falciola, G. and Fresta, F. (1999). Estimation of the non-linear suspension tyre cornering forces from experimental road test data. *Vehicle System Dynamics*, **31**, 23–34.

Kiencke, U., Daiβ, A. (1997). Observation of lateral vehicle dynamics. *Control Engineering Practice*, **5**, 1145–1150.

Kim, J. (2008). Analysis of handling performance based on simplified vehicle lateral dynamics. *Int. J. Automotive Technology* **9**, **6**, 687–693.

Mancosu, F. and Speziari, D., Ceresa, M. and Sbarbati, P. (1999). A new methodology to get reliable input data for handling simulations. *Tire Science and Technology, TSTCA*, **27**, 176–187.

Stephant, J., Charara, A. and Meizel, D. (2007). Evaluation of sliding model observer for vehicle sideslip angle. *Control Engineering Practice*, **15**, 803–812.

Tseng, H. E. (2001). Dynamic estimation of road bank angle. *Vehicle System Dynamics*, **36**, 307–328.

Gelb, A. (1974). *Applied Optimal Estimation*. MIT Press.

Wong, J. Y. (2001). *Theory of Ground Vehicles*. John Wiley & Sons, Inc. New York.